Chinese Chemical Letters 35 (2024) 109260

Contents lists available at ScienceDirect

Chinese Chemical Letters

journal homepage: www.elsevier.com/locate/cclet

Modification of plasma protein for bioprinting *via* photopolymerization

Wenbi Wu[a,1], Yinchu Dong[a,b,1], Haofan Liu[a,1], Xuebing Jiang[a], Li Li[a], Yi Zhang[a], Maling Gou[a,*]

[a] Department of Biotherapy, Cancer Center and State Key Laboratory of Biotherapy, West China Hospital, Sichuan University, Chengdu 610041, China
[b] Chengdu OrganoidMed Medical Laboratory, West China Health Valley, Chengdu 610043, China

ARTICLE INFO

Article history:
Received 12 September 2023
Revised 26 October 2023
Accepted 27 October 2023
Available online 29 October 2023

Keywords:
Bioprinting
Bioink
Photopolymerization
Plasma
Growth factor

ABSTRACT

Bioprinting is emerging as an advanced tool in tissue engineering. However, there is still a lack of bioinks able to form hydrogels with desirable bioactivities that support positive cell behaviors. In this study, modified plasma proteins capable of forming hydrogels with multiple biological functions are developed as bioinks for digital light processing (DLP) printing. The Plasma-MA (BM) was synthesized *via* a one-pot method through the reaction between the fresh frozen plasma and methacrylic anhydride. The methacrylated levels were observed to influence the physical properties of BM hydrogels including mechanical properties, swelling, and degradation. The photo-crosslinked BM hydrogels can sustainedly release vascular endothelial growth factor (VEGF) and exhibit positive biological effects on cell adhesion and proliferation, and cell functionality such as tube formation of human umbilical vein endothelial cells (HUVECs), and neurite elongation of rat pheochromocytoma cells (PC12). Meanwhile, BM hydrogels can also induce cell infiltration, modulate immune response, and promote angiogenesis *in vivo*. Moreover, the plasma bioinks can be used to fabricate customized scaffolds with complex structures through a DLP printing process. These findings implicate that the modified plasma with growth factor release is a promising candidate for bioprinting in autologous and personalized tissue engineering.

Three-dimensional (3D) bioprinting is emerging as a powerful tool in tissue engineering with the unprecedented advantages in fabricating personalized complex structures [1–6]. Digital light processing (DLP) 3D printing is a light-assisted printing technology that has attracted much attention in tissue engineering [7,8]. DLP 3D printing can create bio-scaffolds with superior resolution and speed through patterned photopolymerization of bioinks layer-by-layer [5,9,10]. Bioinks are the fundamental component of bioprinted scaffolds, which should be photopolymerizable for DLP printing [11]. Currently, various natural polymers have been developed as potential bioinks for light-assisted printing [12,13], such as gelatin [14], collagen [15], hyaluronic acid [16], alginate [17], and silk fibroin [18,19]. These natural prepolymers are biodegradable and can provide a friendly microenvironment for cell growth. However, the biological functions of hydrogels formed by these photopolymerizable bioinks are still unsatisfactory to support positive cell behavior and functionality that are present in native tissues.

In recent years, several strategies have been developed to improve the biological functions of hydrogels formed by natural polymers. As a strategy, different natural polymers have been blended to formulate composite natural hydrogels to better mimic the physical and biochemical properties of the native extracellular matrix (ECM) [12,20-22]. However, the formulation of the polymers needs to be optimized to achieve the desired properties, which is complex and labor-intensive. Additionally, incorporating growth factors into biopolymers has also attracted much attention in providing biochemical cues for cell functionality [23,24]. Nevertheless, the incorporation of a single exogenous growth factor cannot replicate the formulation of the endogenous growth factors under a physiological environment, and the biological functions of these hydrogels are still not ideal for tissue engineering.

Plasma is abundant in natural proteins and endogenous growth factors, such as vascular endothelial growth factor (VEGF), hepatocyte growth factor (HGF), fibroblast growth factor (FGF), nerve growth factor (NGF), and brain-derived neurotrophic factor (BDNF) [25,26]. Notably, the formulation of growth factors and proteins in plasma is close to that of physiological conditions *in vivo*. These growth factors and proteins can be involved in various

* Corresponding author.
E-mail address: goumaling@scu.edu.cn (M. Gou).
[1] These authors contributed equally to this work.

https://doi.org/10.1016/j.cclet.2023.109260
1001-8417/

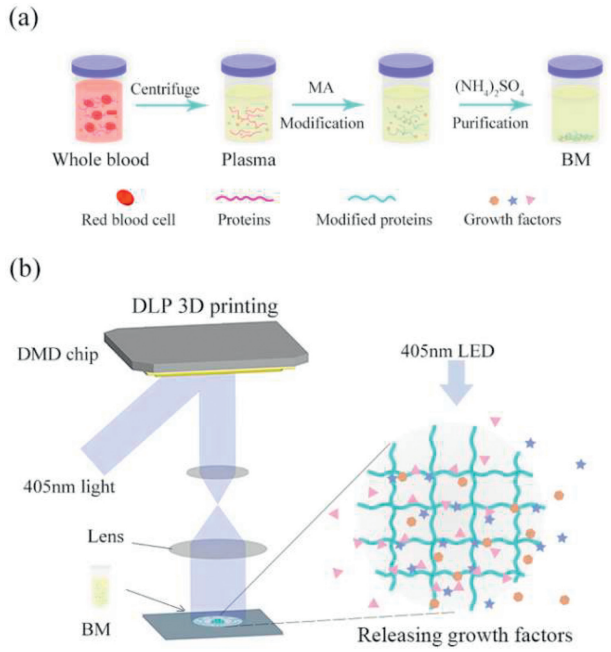

Fig. 1. Plasma bioinks with growth factor release for bioprinting *via* photopolymerization. (a) Schematic illustration of the fabrication of Plasma-MA (BM) by chemical modification with methacryloyl (MA) groups. Plasma was obtained from whole blood by centrifugation, then reacted with methacrylic anhydride, and purified by salting out through ammonium sulfate precipitation. (b) Schematic illustration of DLP printed patterned BM hydrogels with growth factor release.

biological processes, including cell recruitment, and cell survival, proliferation, migration, and differentiation [27]. Plasma exhibits biological functions such as promoting angiogenesis, chondrogenesis, myogenesis, anti-apoptosis, and immunoregulation [25]. It has been demonstrated that plasma has positive effects on tissue regeneration, including cartilage, muscle, nerve, tendon, bone, and skin [25,28-30]. Therefore, plasma is of great potential to be used as a functional bioink for DLP printing in tissue engineering. In our study, we developed photocurable plasma bioinks with growth factor release for DLP 3D printing through modification of fresh frozen plasma (FFP) with methacryloyl (MA) groups (Fig. 1).

Initially, plasma methacryloyl (Plasma-MA, BM) was synthesized through the reaction between methacrylic anhydride (MAA) and the primary amino groups of FFP (Fig. S1 in Supporting information). The reaction was performed in phosphate buffer (PB, pH 7.4) under an ice bath, which was beneficial for maintaining the stability and bioactivity of protein molecules. With different molar ratios of MAA to primary amino group, various BM (BM1, BM2, BM3 and BM4) were prepared, and the degree of substitution (DS) was determined (Table S1 in Supporting information). Subsequently, the methacryloylation was confirmed through ^{1}H nuclear magnetic resonance (NMR) spectroscopy (Fig. 2a). The characteristic peaks of methyl-acrylyl group ($\delta = 5.4$ and 5.6 ppm) and methyl group ($\delta = 1.8$ ppm) appeared upon adding of MAA. Conversely, there was a gradual decrease of the lysine methylene peak at approximately 2.9 ppm with increased MAA amounts, which indicated the substitution of the lysine residues. The modification of MA was further identified by Fourier transform infrared spectroscopy (FTIR) (Fig. 2b). The peaks at 945 and 857 cm^{-1} increased with DS, corresponding to the bending vibration of the methyl-acrylyl group. With the increase of DS, the peak intensity around 1630 cm^{-1} corresponding to the β-sheet decreased gradually, while the intensity of the band around 1660 cm^{-1} representative of the α-helix/random coil increased (Figs. 2c–h). In addition, the overall shape of the amide I band in BM remained unchanged, indicating that BM still maintained a conformation similar to the original plasma. The results demonstrated the synthesis of the MA modified composite biological molecules *via* a mild one-pot method.

Subsequently, BM hydrogels with different DS were formed with prepolymer solution (20% w/v) under exposure to UV light (405 nm), and the physical properties of BM hydrogels were investigated. As shown in Fig. S2a (Supporting information), all BM hydrogel samples exhibited uniform and interconnected porous microstructures, and there was a progressive decrease in the pore size with the increase of DS (Fig. S3 in Supporting information). The mechanical properties of BM hydrogels were evaluated through compressive and tensile tests. The compressive strain decreased with the DS under the same stress (Fig. S2b in Supporting information), while the compressive modulus of BM hydrogel increased gradually with higher DS (Fig. S2c in Supporting information). For tensile property, the increase of DS brought about a decrease in the breaking elongation and an increase in the tensile modulus of hydrogels (Figs. S2d and e in Supporting information). With higher DS, the denser crosslinking may increase the number of polymer chains and make the individual chains shorter, thus improving the stiffness but causing brittleness [31]. Meanwhile, the mass swelling ratio was observed to decrease gradually with increasing DS (Fig. S2f in Supporting information). Besides, BM1, BM2, and BM3 hydrogels were completely degraded after 16 h in 0.25% trypsin solution, while the degradation rate of BM4 was about 90% (Fig. S2g in Supporting information). The results indicated that the physical properties of BM hydrogels could be modulated by DS.

To investigate the biological function of BM hydrogels, we evaluated their effect on human umbilical vein endothelial cells (HUVECs). As shown in Fig. S4 (Supporting information), HUVECs on all hydrogels proliferated and exhibited a spreading morphology with good substrate attachment. The tube formation assay was further performed to evaluate the angiogenic effect of BM hydrogels. Remarkably, HUVECs on BM hydrogels rearranged into interconnected tube-like networks after culture for 18 h (Fig. 3a). Statistical analysis showed that the number of tubes, tube area percentage, and total tube length of BM hydrogels were significantly higher than those of GelMA hydrogel (Figs. 3b–d). Besides, the number of junctions in the BM1, BM2, and BM3 groups was impressively greater than that in the GelMA group (Fig. 3e). The results demonstrated that BM hydrogels with various DS were biocompatible and could promote tube formation of HUVECs. Based on the results, BM2 with a moderate DS was used for further experimental studies.

Vascularization is highly dependent on the biochemical pro-angiogenic microenvironment, especially for the angiogenic factors [32]. There might be bioactive angiogenic factors released from the BM hydrogels. VEGF is one of the key inducers of angiogenesis [32]. To investigate the growth factor release behavior of BM hydrogel, we incubated BM2 hydrogel with PBS buffer (Fig. 3f) and performed an ELISA assay to determine the released VEGF. As shown in Fig. 3g, BM hydrogel exhibited a sustained VEGF release over 42 days. After photopolymerization, the growth factors might be bound with adhesive proteins, physically entrapped, or covalently crosslinked in the BM hydrogel. Through diffusion interaction and hydrogel degradation, the growth factors could be sustainedly released from the BM hydrogel. The sustained release of growth factors would be involved in various biological processes for tissue regeneration [25,28-30].

Plasma contains various proteins and growth factors beneficial for cell proliferation, adhesion, and spreading [26]. The effect of plasma hydrogels on the proliferation and morphology of NIH/3T3 cells was investigated. The proliferation of NIH/3T3 cells on BM hydrogel was comparable to that of GelMA hydrogel (Fig. S5a in Supporting information). After culturing for 48 h, NIH/3T3 cells on BM hydrogel gathered to form small clusters, which was significantly

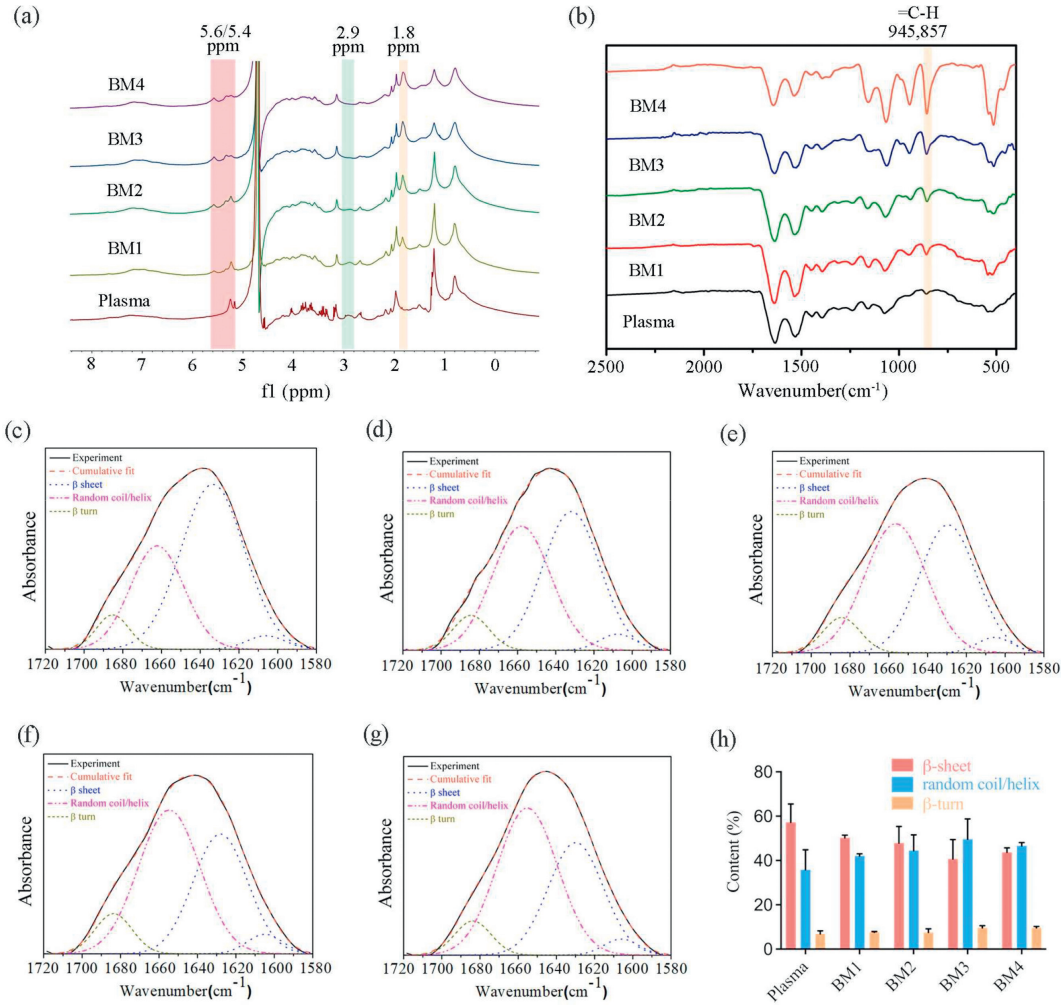

Fig. 2. Characterization of Plasma-MA. (a) ^{1}H NMR of plasma and BM with different DS. (b) FTIR of plasma and BM with different DS. The deconvolution of amide I peak of plasma (c), BM1 (d), BM2 (e), BM3 (f), and BM4 (g). (h) Quantitative analysis of the secondary structures. Data are shown as mean ± standard deviation (SD, $n = 3$).

different from that on GelMA hydrogel (Fig. S5b in Supporting information). To further investigate the effect of BM hydrogel on cell behaviors, we used Schwann cells and rat pheochromocytoma cells (PC12) as models in this study. Schwann cells are the main glial cells of the peripheral nervous system, and PC12 cells can exhibit several neuronal properties [33]. As shown in Figs. S6a–d (Supporting information), Schwann cells and PC12 cells grew well and exhibited more spreading morphologies on BM hydrogels, indicating BM hydrogel was favorable for the adhesion, spreading, and proliferation of cells. Then, rhodamine labeled phalloidin staining was performed to analyze the neurite length of PC12 cells (Fig. S6e in Supporting information). The average neurite length of the BM group (50.92 ± 23.38 μm) was significantly larger than that of the GelMA group (39.34 ± 17.21 μm, $P < 0.001$) and control group (35.09 ± 14.78 μm, $P < 0.001$) (Fig. S6f in Supporting information). The results revealed that BM hydrogel could promote neurite elongation of PC12 cells. It might be due to that the proteins and growth factors, such as insulin-like growth factor 1 (IGF-1), basic fibroblast growth factor (bFGF), transforming growth factor-β (TGF-β), NGF, and glial-derived neurotrophic factor (GDNF), induce the activation of signal pathways that promote neurite outgrowth [34–36]. The results indicated that the BM hydrogels might exhibit positive effects on cell behaviors and functionality.

The biological effect of BM hydrogel *in vivo* was further studied in a subcutaneous implant model (Fig. S8a in Supporting information). The animal experiments were performed in compliance with the guidelines and regulations of West China Hospital of Sichuan University Animal Research Ethics Committee (approval No. 20220712001). GelMA hydrogels were seldom degraded after 1 week, while BM hydrogels were partially degraded (Fig. S7a in Supporting information). Histological analysis showed no inflammatory response in GelMA hydrogel but obvious cell infiltration in BM hydrogel (Fig. S7b in Supporting information). Then, the biodegradation and cell infiltration of BM hydrogel were further investigated (Fig. S8b in Supporting information). As shown in Fig. S8c (Supporting information), cell infiltration could be observed 3 days after implantation, and the infiltrated cells significantly increased at the 7-day timepoint. BM hydrogels still displayed a high density of infiltrated cells at the 14-day timepoint, and almost completely degraded at the 21-day. The infiltrated cells within BM hydrogel were mainly inflammatory cells, possibly related to the immunoregulatory proteins in plasma [26]. Moreover, there were newly formed blood vessels within BM hydrogel at the 7-, 14-, and 21-day timepoints. The results indicated that the biodegradable BM hydrogel could recruit cells, modulate immune response, and promote angiogenesis. Vascularization is crucial for reestablishing or improving blood flow and restoring tissue function in tissue engineering [28]. Meanwhile, the function of the immunomodulatory protein may be advantageous for activating immune response of the body and enhancing the self-healing capacity of injured tissues

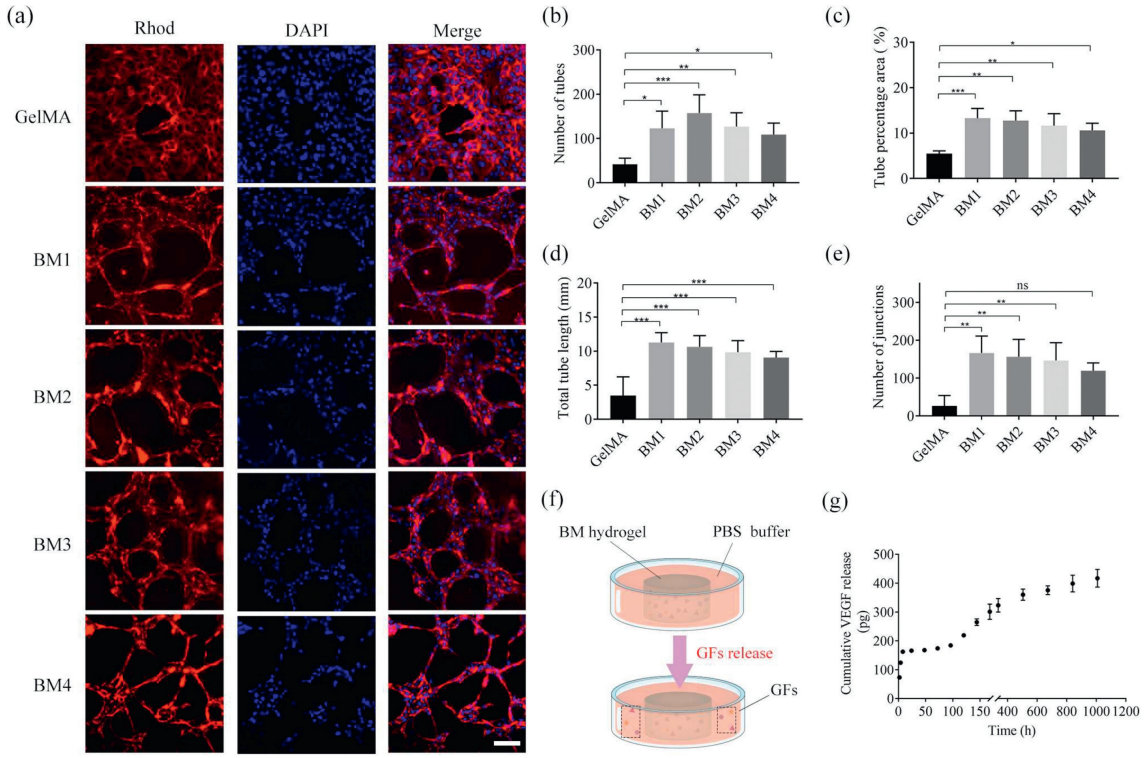

Fig. 3. Tube formation of HUVECs on BM hydrogels and VEGF release from BM hydrogel. (a) Representative images of cytoskeleton staining of HUVECs. Red color represents rhodamine-phalloidin, and blue color represents 4,6-diamino-2-phenyl indole (DAPI). Scale bar: 100 μm. (b) Number of tubes. (c) Tube percentage area. (d) Total tube length. (e) Number of junctions. (f) Schematic illustration of *in vitro* model for growth factor (GF) release. (g) The release profile of VEGF from BM hydrogel. Data are shown as mean ± SD ($n = 3$). $^{*}P < 0.05$, $^{**}P < 0.01$, $^{***}P < 0.001$. ns, $P > 0.05$.

[26]. Therefore, the developed plasma bioinks might be promising candidates for personalized vascularization tissue construction and damaged tissue repair.

To evaluate the printing performance of BM, a series of customized scaffolds were designed and printed. Firstly, the linear arrays were fabricated with high precision and fidelity (Fig. 4a(i)). The line arrays were designed with a width of 15, 25, 35, and 50 μm, respectively, while the actual line width of the printed scaffolds was 13.25 ± 0.27, 24.67 ± 0.81, 34.33 ± 1.37, and 45.50 ± 0.55 μm, respectively. Meanwhile, fluorescein isothiocyanate (FITC) labeled pattern arrays could also be printed with high fidelity (Fig. 4a(ii)), such as triangle array (side length, 200 μm *vs.* 196.18 ± 1.75 μm), square array (side length, 225 μm *vs.* 224.84 ± 2.83 μm), pentagonal array (side length, 225 μm *vs.* 227.71 ± 2.97 μm), and circular array (diameter, 150 μm *vs.* 150.17 ± 2.42 μm). Besides, scaffolds with different shapes were constructed through a continuous DLP printing process (Fig. 4b). A snowflake-like scaffold (1.32 cm in size) and a Sichuan University emblem scaffold (1.81 cm in size) were printed (Fig. 4c(i)). In addition, complex hollow structures were also fabricated by a continuous DLP 3D printing method (Fig. 4c(ii)). BM was demonstrated to be a promising bioink for fabricating complex constructs by DLP 3D printing, which could be useful in bioprinting for personalized tissue engineering.

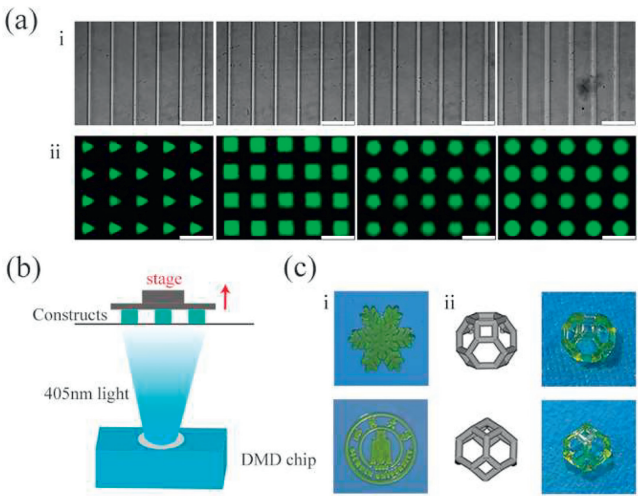

Fig. 4. Printability of BM for DLP printing. (a) Patterned arrays. (i) Linear array structures with the design size of 15, 25, 35 and 50 μm from left to right. Scale bar: 200 μm. (ii) FITC labeled pattern array of triangle, square, pentagon, and circle. Scale bar: 500 μm. (b) Schematic illustration of continuous DLP printing technology. (c) Scaffolds with different shapes. (i) A snowflake-like scaffold and a Sichuan University emblem scaffold. (ii) Complex hollow scaffolds.

In recent years, several studies have investigated the potential of platelet-rich plasma (PRP) and FFP for bioprinting [26,27,37-41]. In these studies, polymers such as alginate, gelatin, or cellulose were often combined with plasma to improve its intrinsic low viscosity. However, plasma itself has not been used as a bioink for bioprinting *via* photopolymerization. In this study, we firstly developed photocurable FFP for DLP printing through a mild one-pot method. We also demonstrated the growth factor release and biological functions of the plasma hydrogels for the first time.

In summary, we developed novel fresh frozen plasma based bioinks for DLP printing through modification with the methacryloyl groups. Such modification allows the production of photocrosslinked BM hydrogels with tunable physical properties. Growth factors such as VEGF could be gradually released from the BM hydrogel. The BM hydrogel could support positive cell behaviors for tissue regeneration such as cell adhesion and proliferation, tube formation of HUVECs, and neurite elongation of PC12 cells. In ad-

dition, the plasma bioinks have good printability to build complex constructs with high precision and fidelity. This functional plasma bioink with growth factor release has the potential for bioprinting *via* photopolymerization for autologous and personalized tissue engineering.

Declaration of competing interest

The authors declare that they have no known competing financial interests or personal relationships that could have appeared to influence the work reported in this paper.

Acknowledgments

This study was supported by the National Natural Science Foundation (No. 32271468); Sichuan Science and Technology Program (No. 2021JDTD0001); Natural Science Foundation of Sichuan Province (No. 2022NSFSC1280); Post-Doctor Research Project, West China Hospital, Sichuan University (No. 2023HXBH081); and Sichuan Science and Technology Program (No. 2021YFS0124). The authors would like to thank Shuping Zheng from the Analytical and Testing Center, Sichuan University, China for the SEM characterization. The authors also appreciated Dr. Ruiqi Dong from National Engineering Research Center for Biomaterials, China for the technical assistance with DMA test. We also thank Boya Li for the help in editing the paper.

Supplementary materials

Supplementary material associated with this article can be found, in the online version, at doi:10.1016/j.cclet.2023.109260.

References

[1] S.V. Murphy, A. Atala, Nat. Biotechnol. 32 (2014) 773–785.
[2] J.T. Toombs, M. Luitz, C.C. Cook, et al., Science 376 (2022) 308–312.
[3] S.N. Sanders, T.H. Schloemer, M.K. Gangishetty, et al., Nature 604 (2022) 474–478.
[4] Y. Chen, J. Zhang, X. Liu, et al., Sci. Adv. 6 (2020) eaba7406.
[5] Y. Sun, K. Yu, Q. Gao, Y. He, Bio-Des. Manuf. 5 (2022) 633–639.
[6] D. Kilian, P. Sembdner, H. Bretschneider, et al., Bio-Des. Manuf. 4 (2021) 818–832.
[7] M. Gou, X. Qu, W. Zhu, et al., Nat. Commun. 5 (2014) 3774.
[8] Y. Huang, W. Wu, H. Liu, et al., Burns Trauma 9 (2021) tkab011.
[9] J. Zhang, Q. Hu, S. Wang, et al., Int. J. Bioprinting 6 (2020) 12–27.
[10] X. Jiang, S. Wang, L. Zhang, et al., Chin. Chem. Lett. 35 (2024) 108686.
[11] A. Sun, X. He, X. Ji, et al., Chin. Chem. Lett. 32 (2021) 2117–2126.
[12] C. Yu, J. Schimelman, P. Wang, et al., Chem. Rev. 120 (2020) 10695–10743.
[13] Y.T. Wang, S. Zhang, J. Wang, Chin. Chem. Lett. 32 (2021) 1603–1614.
[14] H. Shirahama, B.H. Lee, L.P. Tan, N.J. Cho, Sci. Rep. 6 (2016) 31036.
[15] K.E. Drzewiecki, A.S. Parmar, I.D. Gaudet, et al., Langmuir 30 (2014) 11204–11211.
[16] P.A. Levett, F.P. Melchels, K. Schrobback, et al., Acta Biomater. 10 (2014) 214–223.
[17] O. Jeon, K.H. Bouhadir, J.M. Mansour, E. Alsberg, Biomaterials 30 (2009) 2724–2734.
[18] S.H. Kim, Y.K. Yeon, J.M. Lee, et al., Nat. Commun. 9 (2018) 1620–1633.
[19] X. Zhang, W. Wu, Y. Huang, et al., Int. J. Bioprinting 9 (2023) 239–257.
[20] W. Wu, Y. Dong, H. Liu, et al., Mater. Today Bio 20 (2023) 100652.
[21] L. Dong, M. Liang, Z. Guo, et al., Int. J. Bioprinting 8 (2022) 126–139.
[22] F. Fayyazbakhsh, M.J. Khayat, M.C. Leu, Int. J. Bioprinting 8 (2022) 274–291.
[23] J. Tao, H. Liu, W. Wu, et al., Adv. Funct. Mater. 30 (2020) 2004272.
[24] R.S. Hsu, P.Y. Chen, J.H. Fang, et al., Adv. Sci. 6 (2019) 1900520.
[25] E. Anitua, P. Nurden, R. Prado, et al., Biomaterials 192 (2019) 440–460.
[26] T. Ahlfeld, N. Cubo-Mateo, S. Cometta, et al., ACS Appl. Mater. Interfaces 12 (2020) 12557–12572.
[27] N. Faramarzi, I.K. Yazdi, M. Nabavinia, et al., Adv. Healthc. Mater. 7 (2018) 1701347.
[28] E. Anitua, B. Pelacho, R. Prado, et al., J. Control. Release 202 (2015) 31–39.
[29] M. Sanchez, E. Anitua, J. Azofra, et al., Arthroscopy 26 (2010) 470–480.
[30] E. Anitua, G. Orive, J. Control. Release 157 (2012) 317–320.
[31] D. Chimene, R. Kaunas, A.K. Gaharwar, Adv. Mater. 32 (2020) e1902026.
[32] T. Gorski, K. De Bock, Vasc Biol. 1 (2019) H1–H8.
[33] D. Zhang, S. Wu, J. Feng, et al., Acta Biomater. 74 (2018) 143–155.
[34] P.J. Apel, J. Ma, M. Callahan, et al., Muscle Nerve 41 (2010) 335–341.
[35] Y. Koriyama, K. Homma, K. Sugitani, et al., Neurochem. Int. 50 (2007) 749–756.
[36] H. Narai, I. Nagano, H. Ilieva, et al., J. Neurosci. Res. 82 (2005) 452–457.
[37] M. Gruene, A. Deiwick, L. Koch, et al., Tissue Eng. Part C: Methods 17 (2011) 79–87.
[38] N. Cubo, M. Garcia, J.F. del Canizo, et al., Biofabrication 9 (2017) 015006.
[39] B.B. Mendes, M. Gomez-Florit, A.G. Hamilton, et al., Biofabrication 12 (2019) 015012.
[40] L. Wei, S. Wu, M. Kuss, et al., Bioact. Mater. 4 (2019) 256–260.
[41] S.J. Min, J.S. Lee, H. Nah, et al., Biofabrication 13 (2021) 044102.